MNRAS **000**, 1–?? (2016) Preprint 19 January 2017 Compiled using MNRAS LATEX style file v3.0

An upper limit on the masses of ultra diffuse galaxies from weak gravitational lensing

Cristóbal Sifón[1,2], Remco F. J. van der Burg[3], Henk Hoekstra[2] Adam Muzzin[4] and Ricardo Herbonnet[2]

[1]*Department of Astrophysical Sciences, Peyton Hall, Princeton University, Princeton, NJ 08544, USA*
[2]*Leiden Observatory, Leiden University, PO Box 9513, NL-2300 RA Leiden, Netherlands*
[3]*Laboratoire AIM, IRFU/Service d'Astrophysique - CEA/DSM - CNRS - Université Paris Diderot, Bât. 709, CEA-Saclay, 91191 Gif-sur-Yvette Cedex, France*
[4]

19 January 2017

ABSTRACT

The recent discovery of thousands of ultra diffuse galaxies (UDGs) in nearby galaxy clusters has opened a new window into the process of galaxy formation and evolution. Among the key features that could reveal their formation history and ability to survive in the harsh cluster environments are the masses of these UDGs. We use weak gravitational lensing measurements around 909 UDGs in 21 clusters at $z \leq 0.09$ to constrain the average total mass of UDGs. We constrain the average mass of subhaloes hosting UDGs to $\log m_{\rm UDG}/{\rm M}_\odot \leq 11.45$, within a radius $r \sim 40$ kpc, at 95 per cent confidence. Although uncertainties are large, our lensing measurements suggest that UDGs are dwarfs and not failed L^* galaxies.

1 INTRODUCTION

Large, low surface brightness galaxies have been known to exist both in the field () and in galaxy clusters () for some time. **their properties etc.**

A subset of these low surface brightness galaxies—dubbed ultra-diffuse galaxies (UDGs) by van Dokkum et al. (2015a)—has recently started receiving particular attention. These UDGs are large ($r_{\rm eff} \geq 1.5$ kpc, where $r_{\rm eff}$ is the half-light radius), low-surface brightness galaxies (with central surface brightnesses $\mu_0 \sim 26-28$ mag arcsec^{-2}) initially discovered in the Coma Cluster (van Dokkum et al. 2015a; Koda et al. 2015; Yagi et al. 2016), and later in Virgo (Mihos et al. 2015) and Fornax (Muñoz et al. 2015), and even in a number of more distant ($0.04 \leq z \leq 0.07$) clusters (van der Burg et al. 2016). UDGs have dwarf-like stellar masses, $M_\star \sim 10^8$ M$_\odot$ (e.g., van der Burg et al. 2016), but sizes comparable to the Milky Way, which has a total mass $M \sim 10^{12}$ M$_\odot$.

Several hypotheses have been put forth to try to explain the unexpected survival of UDGs in massive clusters. In the initial discovery of UDGs in the Coma Cluster, van Dokkum et al. (2015a) suggested that UDGs may be failed L^* galaxies which fell into the cluster at early times, after having used only a small fraction of their cold gas to form stars. Once part of a cluster, their remaining cold gas was removed and they were left as very dark matter dominated galaxies. Yozin & Bekki (2015) have shown that such a mechanism can in fact produce UDG-like galaxies in hydrodynamical simulations. Alternatively, Amorisco & Loeb (2016) and Di Cintio et al. (2017) have suggested that the intrinsic properties of some dwarf galaxies are responsible for the formation of UDGs; they should therefore be abundant in the field. However, a study of UDGs in the field is complicated by the lack of redshift information, whereas large numbers of UDGs that happen to be co-located in projection with galaxy clusters can safely be assumed to be part of the cluster (or at least a significant fraction of them; e.g., van der Burg et al. 2016). Furthermore, the one UDG with a spectroscopic redshift has been confirmed to be part of the Coma cluster (van Dokkum et al. 2015b).

If there is one quantity which plays a crucial role in the distinction between these different sets of hypothesis, it is arguably the total masses of UDGs. Knowing the masses of UDGs would allow us to unambiguously rule out some classes of hypotheses as those summarized above. There have already been attempts at estimating the masses of individual UDGs. Beasley et al. (2016) measured a velocity dispersion of globular clusters associated with a UDG in the Virgo Cluster of 33^{+16}_{-10} km s^{-1} within 8.1 kpc, which suggests a virial mass[1] $m_{200} \sim 10^{11}$ M$_\odot$. Similar values for the total masses of UDGs have been obtained from the number of globular clusters (Beasley & Trujillo 2016; Peng & Lim 2016). All these measurements therefore suggest that UDGs are in fact dwarf galaxies and not failed L^* galaxies. On the other hand, van Dokkum et al. (2016) estimated a virial mass $m \sim 10^{12}$M$_\odot$ from the stellar velocity dispersion and globular cluster count of a large ($r_{\rm eff} = 4.5$ kpc) UDG, comparable to the mass of the Milky Way—possibly a failed L^* galaxy. Since all of the above mass estimations refer to single UDGs, it is not clear how they can be interpreted in the context of the UDG population. For this reason, measurements of the masses of a representative population of UDGs are required to draw conclusions about their origin.

Only weak gravitational lensing can provide direct measure-

[1] Note that subhaloes cannot be physically assigned a virial mass, since they are embedded in the potential of the host cluster. However, referring to virial masses offers a convenient point for comparison. We therefore adhere to the use of virial masses in this discussion, but adopt a different mass definition in our analysis (see Section 3). See also the discussion in Sifón et al. (2017).

© 2016 The Authors

Table 1. Cluster sample. Clusters masses, M_{200}, refer to the dynamical masses estimated by Sifón et al. (2015b), and r_{200} are the radii containing such masses. Note that here the overdensity is defined with respect to the critical density of the Universe. The last two columns list the number of good UDG candidates after cleaning the sample by visual inspection, uncorrected for possible interlopers, and the estimated number of interlopers in parentheses.

Cluster	Redshift	M_{200} ($10^{14}\mathrm{M}_\odot$)	r_{200} (Mpc)	Number of UDGs
A85	0.055	10.2 ± 1.8	2.0 ± 0.1	97
A119	0.044	7.4 ± 1.2	1.8 ± 0.1	82
A133	0.056	5.5 ± 1.6	1.7 ± 0.2	78
A399	0.072	6.6 ± 2.0	1.8 ± 0.2	63
A401	0.074	8.9 ± 2.3	1.9 ± 0.2	57
A780	0.055	7.2 ± 2.7	1.8 ± 0.2	57
A1650	0.084	4.5 ± 0.9	1.5 ± 0.1	16
A1651	0.085	8.0 ± 1.3	1.9 ± 0.1	35
A1781	0.062	0.6 ± 0.3	0.8 ± 0.1	20
A1795	0.063	5.0 ± 0.9	1.6 ± 0.1	109
A1991	0.059	1.9 ± 0.5	1.2 ± 0.1	35
A2029	0.078	16.1 ± 2.5	2.4 ± 0.1	34
A2033	0.080	7.7 ± 2.0	1.8 ± 0.2	25
A2064	0.073	3.4 ± 1.7	1.4 ± 0.2	5
A2065	0.072	14.4 ± 2.5	2.3 ± 0.1	19
A2142	0.090	13.8 ± 1.2	2.2 ± 0.1	62
A2495	0.079	4.1 ± 0.8	1.5 ± 0.1	13
A2597	0.083	3.5 ± 2.0	1.4 ± 0.3	20
A2670	0.076	8.5 ± 1.2	1.9 ± 0.1	26
MKW3S	0.045	2.6 ± 0.5	1.3 ± 0.1	23
ZWCL1215	0.077	7.7 ± 1.7	1.9 ± 0.1	33

ments of *typical* masses of UDGs. Because lensing does not rely on faint, low-surface brightness baryonic tracers of the mass in galaxies, it provides a clear advantage over stellar dispersion measurements or globular cluster counts.

In this work, we present weak gravitational lensing measurements of the masses of UDGs in a sample of 21 clusters at $z < 0.1$ taken from the Multi-Epoch Nearby Cluster Survey (MENeaCS). We present the data and summarize the weak lensing formalism in Section 2. We discuss the modelling of the signal and the resulting constraints on UDG masses in Section 3, and discuss the implications of our measurements in Section 4. Throughout this work we adopt a flat ΛCDM model with $\Omega_\mathrm{m} = 0.315$ and $H_0 = 70\,\mathrm{km\,s^{-1}Mpc^{-1}}$, consistent with the latest results of the *Planck* satellite (Planck Collaboration 2015).

2 DATA ANALYSIS

2.1 UDG sample

MENeaCS is a multi-epoch survey of 57 clusters at $z \leq 0.15$ carried out with Megacam in the Canada-France-Hawaii Telescope (Sand et al. 2012). The data reduction is described in detail by van der Burg et al. (2013). The resulting full width at half maximum of the point spread function is less than 1 arcsec for all clusters in the sample, and the photometric zero points have been calibrated to about 0.01 mag. We consider 21 of those 57 clusters, located at $z \leq 0.09$. These clusters have masses $M_{200} \gtrsim 10^{14}\,\mathrm{M}_\odot$, where M_{200} is the dynamical mass estimated by Sifón et al. (2015b). Our cluster sample is listed in Table 1.

Following the original definition by van Dokkum et al. (2015a), van der Burg et al. (2016) identified UDGs as galaxies with surface brightnesses within one effective radius of $24.0 \leq \langle\mu(r, r_\mathrm{eff})\rangle \leq 26.5$ and effective radii $1.5 \leq r_\mathrm{eff}/\mathrm{kpc} \leq 7.0$; these parameters were measured with GALFIT (Peng et al. 2002, 2010). In order to have a sample that is as pure as possible but still obtain a large enough number of UDG candidates, van der Burg et al. (2016) considered eight clusters at $0.04 \leq z \leq 0.07$ and at galactic latitude $b \geq 25°$. The study of van der Burg et al. (2016) is unique in that they did not select UDGs by visual inspection after the automatic selection based on structural parameters. While this has the disadvantage that the sample may be (and in fact is, as we show below) contaminated by artefacts of various kinds, it allows for an objective, statistically-consistent study of their properties after accounting for the expected number of such objects in control fields. This contamination however can significantly alter lensing measurements in a way that may not be fully captured by subtracting the signal from a control sample.

We start from the sample compiled by van der Burg et al. (2016), but take some additional steps to define the sample used for weak lensing measurements. We first expand the cluster sample to $z \leq 0.09$ in order to increase the number of UDGs in our sample. We also impose stricter size cuts on the UDG sample $r_\mathrm{eff} \geq 2.0\,\mathrm{kpc}$ for $z \leq 0.065$ and $r_\mathrm{eff} \geq 3.0\,\mathrm{kpc}$ for higher redshifts, as we find that these cuts significantly reduce the contamination of the sample. Finally, we visually inspected all UDG candidates and only kept high-confidence UDG candidates. We classify a UDG candidate as high-confidence if it is unambiguously an isolated galaxy whose GALFIT parameters are expected to be accurate (i.e., without significant residuals in a model-subtracted image), but do not make any visual selection based on surface brightness or morphology. While this slightly subjective selection could potentially bias statistical analyses such as that carried by van der Burg et al. (2016), it is essential for a clean interpretation of lensing measurements around the UDGs. We show the distribution of stellar mass of our final sample of UDGs in Figure 1.

2.2 Weak lensing measurements

Our weak lensing analysis is identical in methodology to that presented in Sifón et al. (2017), which follows closely the analysis of Hoekstra et al. (2015). The weak lensing signal is measured as an average tangential alignment, or shear, γ_t, of galaxies in the background of the lenses (in this case, UDGs) using the moments-based KSB algorithm (Kaiser et al. 1995; Luppino & Kaiser 1997; Hoekstra et al. 1998). The shear is closely related to the excess surface density, $\Delta\Sigma$,

$$\Delta\Sigma \equiv \bar{\Sigma}(< R) - \bar{\Sigma}(R) = \Sigma_\mathrm{c}\gamma_\mathrm{t}, \quad (1)$$

where $\bar{\Sigma}(< R)$ and $\bar{\Sigma}(R)$ are the average surface densities within a projected radius[2] R and within a thin shell around R, respectively, and Σ_c is a geometric factor accounting for the lensing efficiency,

$$\Sigma_\mathrm{c} \equiv \frac{c^2}{4\pi G}\frac{D_\mathrm{s}}{D_\mathrm{l}D_\mathrm{ls}}, \quad (2)$$

with D_s, D_l and D_ls being the angular diameter distances to the source, to the lens, and between the lens and the source.

We define our source sample in an identical way to Sifón et al. (2017). As in Sifón et al. (2017), we do not apply any colour cuts, but correct the lensing measurements with a 'boost factor' that accounts for contamination by cluster members. This boost factor has

[2] As a convention, we list two-dimensional distances with upper case R and three-dimensional distances with lower case r.

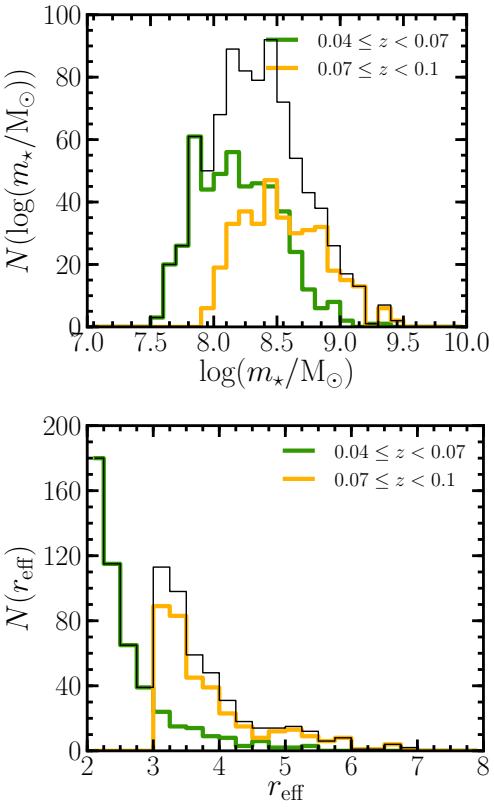

Figure 1. Distribution of stellar masses (top) and effective radii (bottom) of the UDG candidates that pass our visual inspection, split into a low (green) and high (orange) redshift samples. The thin black lines show the distribution for the full sample.

been caibrated using tailor-made image simulations. In addition, Sifón et al. (2017) used the same image simulations to describe and account for an additive bias in the tangential shear due to the light from the lens galaxies. The lens sample of Sifón et al. (2017) is composed of typical, bright ($m_\mathrm{phot} = 14 - 20$) cluster galaxies, and this additive correction is significant but confined to very small scales ($R < 50\,\mathrm{kpc}$). However, it is entirely negligible for UDGs, given their low surface brightness.

3 THE WEAK LENSING SIGNAL OF ULTRA DIFFUSE GALAXIES

3.1 Model for the UDG lensing signal

As described in detail in Yang et al. (2006) and Sifón et al. (2015a), the satellite lensing signal can be described by the sum of a subhalo and a host halo terms, both of which are essentially independent of each other. We model the average density profile of both UDGs and the host clusters as NFW profiles (Navarro et al. 1995). Following Sifón et al. (2017), we define the mass of subhaloes hosting UDGs, m_bound, as the bound subhalo mass—that is, the mass within the region where the density is above the background density of the cluster. In order to estimate the background density, we take the expected value for the three-dimensional radius based on the number density profile of normal cluster galaxies measured by van der Burg et al. (2015), which provides a good description of the distribution

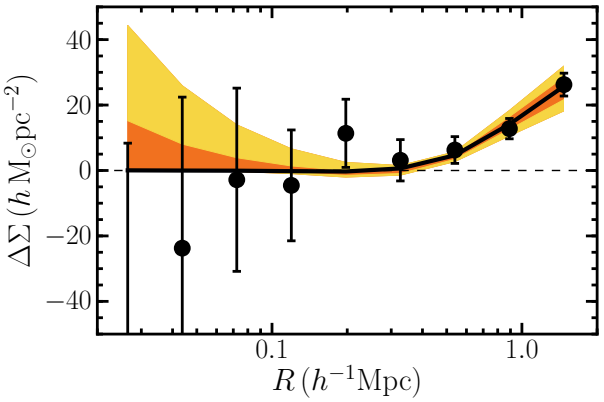

Figure 2. Lensing signal of ultra-diffuse galaxies in clusters at $z \leq 0.09$. Orange and yellow regions show the 68 and 95 per cent credible intervals from the MCMC sampling, while the black line shows the best-fit model.

of UDGs outside $R_\mathrm{sat} \sim 0.15 r_{200}$. Specifically,

$$\langle r_\mathrm{UDG}\rangle = \left[\int_{0.15c}^{c} d\chi\,\rho(\chi,c)\right]^{-1} \int_{0.15c}^{c} d\chi\,\chi\,\rho(\chi,c) = 0.38 r_{200,\mathrm{h}}\,, \qquad (3)$$

where $\rho(x,c)$ is the NFW profile and $c = 2$ (van der Burg et al. 2015, 2016). Our model therefore has four free parameters: the average masses and concentrations of UDGs and the corresponding ones for host clusters. In practice, we are only able to constrain the masses of UDGs and their host clusters; we treat the concentrations as nuisance parameters.

3.2 Constraints on the average UDG mass

We show in Figure 2 the lensing signal of our sample of UDGs, along with the best-fit model. We are not able to constrain the concentrations of either UDGs or the host clusters, and we marginalize over the concentration parameters. For UDGs we use a range $10 \leq c_\mathrm{UDG} \leq 20$, which covers the expected average concentrations of subhaloes in the mass range $\log m/\mathrm{M}_\odot \sim 10 - 12$ and at cluster-centric distances $0.1 \lesssim r/r_{200,\mathrm{cl}} \lesssim 1$ (Moliné et al. 2016). Similarly, we set $2 \leq c_\mathrm{cl} \leq 8$ for the host clusters (e.g., Dutton & Macciò 2014).

Our model constrains the 'virial' mass of subhaloes to $\log m_{200}/\mathrm{M}_\odot \leq 11.94$ at 95 per cent credibility. At an average cluster-centric distance of $\langle r_\mathrm{UDG}\rangle = 0.38 r_{200,\mathrm{cl}}$, this results in a bound mass $\log m_\mathrm{bound}/\mathrm{M}_\odot \leq 11.45$ within a radius $r_\mathrm{bound} = 41^{+41}_{-37}$ kpc at 95 per cent credibility. The wide range in r_bound is given by the range in allowed host cluster masses, which changes both the background density and the value of $r_{200,\mathrm{cl}}$. The best-fit host cluster mass is $\log M_\mathrm{cl}/\mathrm{M}_\odot = 14.96^{+0.11}_{-0.11}$ (68 per cent credible interval).

These results are somewhat dependent on the range chosen for c_UDG, with lower concentrations allowing for higher subhalo masses. However, it is unlikely that subhaloes would have concentrations much lower than $c = 10$—these are in fact the typical concentrations of *host* haloes of these masses (e.g., Dutton & Macciò 2014; Moliné et al. 2016).

To allow a comparison with recent measurements of UDG masses from stellar dynamics and globular clusters, we also report the upper limit for the mass within 10 kpc, $m_{<10\,\mathrm{kpc}} \leq XX\,\mathrm{M}_\odot$, but we note that this value is an extrapolation of the data—a result of the adopted NFW profile.

4 DISCUSSION

Weak gravitational lensing measures the total mass irrespective of its nature. The median stellar mass of UDGs in our sample is $\langle m_\star \rangle = 2.0 \times 10^8\,\mathrm{M}_\odot$. Thus their dark matter fraction can be as high as 99.9 per cent, although we are not able to detect mass in excess of the stellar mass. Lensing has the advantage compared to stellar dynamics that it probes the total masses of galaxies, instead of the masses within the small radii within which velocity dispersions can be measured (e.g., roughly 8 kpc in the case of DF17 in the Coma cluster Beasley & Trujillo 2016; Peng & Lim 2016), and therefore allows a more straightforward comparison with other kinds of galaxies, without the need for an extrapolation of the density profile from ~ 8 kpc to tens of kpc (although lensing also relies to some extent on an assumed density profile).

However, weak lensing has therefore the disadvantage that the total and stellar masses are measured at very different radii, and the question of how dark matter–dominated these galaxies are, compared to dwarf or 'normal' galaxies, is difficult to address.

Our weak lensing measurements suggest the typical UDG (with $\langle r_\mathrm{eff} \rangle \sim 3$ kpc) resides in a dark matter halo that contains at most half the mass of the Milky Way. This supports the idea that UDGs are dwarfs, as opposed to failed L^* galaxies. This is in agreement with the mass suggested by globular cluster counts in a $r_\mathrm{eff} = 2.5$ kpc UDG in the Coma cluster (Beasley & Trujillo 2016; Peng & Lim 2016). On the other hand, van Dokkum et al. (2016) estimated a virial mass of about $10^{12}\,\mathrm{M}_\odot$ for DF44 (also in Coma). This UDG has a stellar mass $m_\star \sim 3 \times 10^8\,\mathrm{M}_\odot$, similar to the average stellar mass in our sample, but an effective radius $r_\mathrm{eff} \sim 4.5$ kpc, not representative of UDGs in general. The total mass inferred by van Dokkum et al. (2016) suggests either that DF44 is an outlier, *compared to the population of UDGs*, in terms of its total-to-stellar mass ratio, or that the assumed extrapolation from a dynamical mass of $7 \times 10^9\,\mathrm{M}_\odot$ within 4.6 kpc to a virial mass of $\sim 10^{12}\,\mathrm{M}_\odot$ is not valid. For this extrapolation, van Dokkum et al. (2016) assumed a concentration of $c \sim 10$ (Macciò et al. 2008), at the low end of our chosen range. As discussed above, lowering the concentration tends to increase the mass allowed by our lensing measurements, and this may partly explain the fact that we consider DF44 an outlier. A study of the velocity dispersion of a statistical sample of UDGs may help understand this difference.

Our upper limit on the mass of UDGs suggests that they are not strong outliers in the total-to-stellar mass relation of cluster galaxies, as measured by Sifón et al. (2017). So far, theoretical scenarios in which UDGs are dwarf galaxies also require an abundant field UDG population. A study of field UDGs would face the additional challenge that it would be very difficult to determine their redshifts in large numbers.

make plot like right panel of fig 8 with the UDG upper limit

REFERENCES

Amorisco N. C., Loeb A., 2016, MNRAS, 459, L51
Beasley M. A., Trujillo I., 2016, preprint, (arXiv:1604.08024)
Beasley M. A., Romanowsky A. J., Pota V., Navarro I. M., Martinez Delgado D., Neyer F., Deich A. L., 2016, ApJL, 819, L20
Di Cintio A., Brook C. B., Dutton A. A., Macciò A. V., Obreja A., Dekel A., 2017, MNRAS, 466, L1
Dutton A. A., Macciò A. V., 2014, MNRAS, 441, 3359
Hoekstra H., Franx M., Kuijken K., Squires G., 1998, ApJ, 504, 636
Hoekstra H., Herbonnet R., Muzzin A., Babul A., Mahdavi A., Viola M., Cacciato M., 2015, MNRAS, 449, 685
Kaiser N., Squires G., Broadhurst T., 1995, ApJ, 449, 460
Koda J., Yagi M., Yamanoi H., Komiyama Y., 2015, ApJL, 807, L2
Luppino G. A., Kaiser N., 1997, ApJ, 475, 20
Macciò A. V., Dutton A. A., van den Bosch F. C., 2008, MNRAS, 391, 1940
Mihos J. C., et al., 2015, ApJL, 809, L21
Moliné Á., Sánchez-Conde M. A., Palomares-Ruiz S., Prada F., 2016, preprint, (arXiv:1603.04057)
Muñoz R. P., et al., 2015, ApJL, 813, L15
Navarro J. F., Frenk C. S., White S. D. M., 1995, MNRAS, 275, 720
Peng E. W., Lim S., 2016, ApJL, 822, L31
Peng C. Y., Ho L. C., Impey C. D., Rix H.-W., 2002, AJ, 124, 266
Peng C. Y., Ho L. C., Impey C. D., Rix H.-W., 2010, AJ, 139, 2097
Planck Collaboration 2015, preprint, (arXiv:1502.01589)
Sand D. J., et al., 2012, ApJ, 746, 163
Sifón C., et al., 2015a, MNRAS, 454, 3938
Sifón C., Hoekstra H., Cacciato M., Viola M., Köhlinger F., van der Burg R. F. J., Sand D. J., Graham M. L., 2015b, A&A, 575, A48
Sifón C., Herbonnet R., Hoekstra H., Cacciato M., van der Burg R. F. J., Viola M., Sand D. J., Graham M. L., 2017, in preparation
Yagi M., Koda J., Komiyama Y., Yamanoi H., 2016, ApJS, 225, 11
Yang X., Mo H. J., van den Bosch F. C., Jing Y. P., Weinmann S. M., Meneghetti M., 2006, MNRAS, 373, 1159
Yozin C., Bekki K., 2015, MNRAS, 452, 937
van Dokkum P. G., Abraham R., Merritt A., Zhang J., Geha M., Conroy C., 2015a, ApJL, 798, L45
van Dokkum P. G., et al., 2015b, ApJL, 804, L26
van Dokkum P., et al., 2016, preprint, (arXiv:1606.06291)
van der Burg R. F. J., et al., 2013, A&A, 557, A15
van der Burg R. F. J., Hoekstra H., Muzzin A., Sifón C., Balogh M. L., McGee S. L., 2015, A&A, 577, A19
van der Burg R. F. J., Muzzin A., Hoekstra H., 2016, A&A, 590, A20